Hemispheric Asymmetry of Globus Pallidus Explains Reward-related Posterior Alpha Modulation in Humans

Subcortical modulation of visual alpha oscillations

C. Mazzetti[1], T. Staudigl[1], T. R. Marshall[3], J. M. Zumer[2,4], S. J. Fallon[3] & O. Jensen[4]

[1] Donders Institute for Brain, Cognition and Behaviour, Radboud University, Nijmegen, The Netherlands;

[2] School of Psychology, University of Birmingham, Birmingham, UK;

[3] Department of Experimental Psychology, University of Oxford, UK;

[4] Centre for Human Brain Health, School of Psychology, University of Birmingham, Birmingham, UK;

Corresponding author: Cecilia Mazzetti, Donders Institute for Brain, Cognition and Behaviour, Radboud University Nijmegen, P.O. Box 9101, NL-6500 HB Nijmegen, The Netherlands; phone: +31-24-36- 65059; email: c.mazzetti@donders.ru.nl

Abstract

Although basal ganglia (BG) functions have been widely explored in relation to motor control, recent evidence suggests that their mechanisms extend to the domain of attentional switching. We here investigated the BG involvement in reward related top-down control of visual alpha-band oscillations (8 – 13 Hz), which have been linked to the mechanisms supporting the allocation of spatial attention. Given that items associated with contextual saliency (e.g. monetary reward or loss) attract attention, it is not surprising that alpha oscillations are further modulated by the saliency properties of the visual items. The executive network controlling such reward-dependent modulations of oscillatory brain activity has yet to be elucidated, and likely relies on the contribution of subcortical regions. To uncover this, we investigated whether derived measures of basal ganglia (BG) structural asymmetries could predict interhemispheric modulation of alpha power, during a spatial attention task. We show that volumetric lateralization of the globus pallidus (GP) significantly explains individual hemispheric biases in alpha power modulation. Importantly, this effect varied as a function of value-saliency parings in the task. We hence provide compelling evidence suggesting that the GP in humans is a node within the executive control network, implicated in reward related top-down control of visual alpha oscillations during saliency processing.

Introduction

While basal ganglia (BG) involvement in motor planning and execution has been extensively described [1–4], growing evidence points to their role extending to higher level cognitive functions. This notion has been already explored in animal recordings [5–8], with fewer studies reporting BG cognitive control in humans. Among these, it has recently been suggested that the BG nuclei play a role in spatial attention and selection [9–11]. This hypothesis has been investigated with a particular emphasis on reward-related saliency processing [12–15]. Consistent to this notion, volumetric abnormalities related to the BG have been associated with symptoms of inattention in attention deficit and hyperactivity disorder (ADHD) [16–18] together with aberrant salience attribution in schizophrenia [19–23].

In order to efficiently operate in natural environments, our brains must rely on neuronal mechanisms which selectively gate stimuli by prioritizing relevant information whilst reducing the interference of distractors [24]. In particular, deployment of attentional resources is biased towards stimuli associated with salience (e.g. monetary reward or loss), even when unrelated to the current task goals[25]. Converging evidence has shown that modulations of posterior neuronal oscillations in the alpha band (8 – 13 Hz) reflect the allocation of covert attention [26–28]. In particular, a selective suppression of alpha-band oscillations is observed over visual areas contralateral to the attended hemifield, while a relative increase occurs ipsilaterally [28]. It is now clear that the dorsal attention network (DAN) plays a crucial role in the modulation of alpha band activity in spatial attention tasks [29–33]; however, the involvement of subcortical regions is yet to be fully uncovered. In particular, it still has to be elucidated whether the BG – in coordination with the DAN – exert influence over the top-down control of posterior alpha band oscillations.

Activity from the BG is not likely to be detectable with Magnetoencephalography (MEG) due to the lower sensitivity of the technique to deeper structures in the brain. As an alternative, recent studies have succeeded in relating structural brain properties to the ability to modulate oscillatory brain activity [34,35]. For instance, a recent study exploited individual hemispheric asymmetries in the volume of the superior longitudinal fasciculus (SLF) [31], a white matter tract connecting fronto-parietal regions, supposedly involved in top-down visuospatial attention. Importantly, the study demonstrated that subjects with greater right than left SLF volume were also the ones displaying higher modulation of posterior alpha activity in the left hemisphere, compared to the right (and vice versa). Through an analogous approach, we postulated that volumetric asymmetries of the BG nuclei would be reflected by individual interhemispheric biases in the modulation of alpha oscillations during selective attention in a reward context, given the well-established role of these nuclei into reward processing and salience attribution. We here implicitly established the assumption that a bigger subcortical volume would exercise better control over alpha oscillations.

To investigate this hypothesis we made use of data from a recent study that considered the impact of stimuli paired with value salience on the modulation of oscillatory brain activity in a covert attention task [36]. MEG data were recorded while participants performed a spatial cueing task in which Chinese symbols served as targets and distractors. Prior to the recordings, stimuli were paired with monetary rewards or losses. This alpha power modulation was shown to be influenced by the salience of the targets and distractors, but not their valence (i.e., reward and loss had the same effect). We here re-analysed these data with the aim to investigate the putative role of the BG in biasing alpha power modulation during attentional shifts to stimuli paired with value-saliency. Magnetic Resonance Imaging (MRI) data of the same participants were processed in order to estimate volumetric asymmetries of BG structures. We focused on identifying the link between individual volumetric

asymmetries of the BG and individual interhemispheric bias in the ability to modulate posterior alpha oscillations. Crucially, we examined whether this relationship was affected by the degree of stimulus-value associations in the task [37].

Results

We acquired structural and electrophysiological data from 25 participants. Participants' performance was tested during a covert attention paradigm, where Chinese symbols served as targets and distractors (Figure 1). During a learning phase, prior to the actual task, the stimuli were associated with different values (positive, negative or neutral). In the testing phase, a central cue probed the imminent contrast variation of the target, which appeared either at 1450 or 2350 ms, predicting its position in 95% of the trials. Participants were instructed to indicate, with button press, the direction of the contrast change, which could either increase or decrease with equal probability.

MEG data were acquired during the testing phase and related time-frequency representations of power were derived. Indices of power modulation (MI) were computed by contrasting frequency power in trials where participants were validly cued to the right (*attend right* trials) with trials where participants were validly cued to the left (*attend left* trials) (see Eq.(1), *Materials and Methods*). Consistent with previous results, participants displayed a clear modulation of alpha band activity at parieto-occipital sensors (MI(α)): when covertly orienting attention to a cued side, alpha power decreased in the contralateral hemisphere while it increased relatively in the ipsilateral hemisphere (Figure 2A). The magnitude of alpha power modulation, as reflected by MI(α), progressively increased until the target changed contrast (Figure 2B). To encompass this increase, we focused our analysis on the 750 ms interval immediately preceding the onset of the contrast change. Next, right and left ROIs were identified as clusters of symmetric pairs of sensors showing the highest alpha lateralization (see *Materials and Methods*).

In order to quantify the magnitude of hemispheric alpha modulation bias, Hemispheric Lateralized Modulation of alpha power (HLM(α)) values were then computed for each

participant by summing the average MI(α) in the right and left hemisphere ROIs (see Eq.(2), *Materials and Methods*): positive HLM(α) values indicate stronger modulation of absolute alpha power in the left compared to the right hemisphere, and vice versa. The histogram in Figure 2B depicts the distribution of hemispheric bias related to attentional modulation of alpha power. HLM(α) indices were normally distributed around zero across participants (Shapiro Wilk, $W = .958$, $p = .392$).

Volumetric asymmetry of basal ganglia in relation to hemispheric lateralized alpha modulation

We sought to determine whether HLM(α) values related to covert attentional processes during the task, irrespective of value-salience levels, were predicted by hemispheric asymmetries of the basal ganglia (BG). A semi-automated segmentation tool was used to estimate anatomical volumes for the left and right hemisphere BG: Globus Pallidus (GP), Nucleus Accumbens (NAcc), Caudate (CN) and Putamen (Pu). We then calculated the volumetric asymmetry (LV) for each set of nuclei (see *Materials and Methods,* Eq.(3)). Analogously to HLM indices, positive (or negative) LV_s value indicated that, for a given participant, substructure *s* was left (or right) lateralized. As the assumption of normality was not met for the distribution of LV_{CN} values, a two-sided Wilcoxon signed rank test was applied on LV indices of all substructures. This revealed that, at the group level, the NAcc was significantly left lateralized ($z = -3.78$, $p = .000$) whilst the CN was right lateralized ($z = 2.97$, $p = .003$). For the other substructures, no significant lateralization was found for LV values in the sample. To investigate whether individual subcortical asymmetries predicted differences in hemispheric lateralized modulation of alpha power, we implemented a GLM approach, where HLM(α) indices were set as predictor variable for subcortical structures lateralization (LV_s) derived from Eq(3), defined as the response variable. A significant

regression was found: when considering the grand average of all conditions, a linear combination of the subcortical LVs explained HLM(α) values ($F_{4,20} = 3.81$, $p = .019$, adjusted $R^2 = .319$) (Figure 4A). When assessing each predictor individually, only the beta coefficient for LV_{GP} was found to be significantly greater than zero ($p = .003$). Hence, when controlling for the other explanatory variables in the model, only GP asymmetry (LV_{GP}) significantly explained the hemispheric lateralized alpha band modulation ($\beta = .872$, $p = .003$). The unique contribution of GP lateralization is visible in Figure 4B, showing the partial regression plot between LV_{GP} and HLM(α).

Globus pallidus asymmetry selectively correlates with power modulation in the alpha band

In order to better interpret the GLM results, we assessed whether the linear relationship arising from the model was actually restricted to the alpha band: to this end, a non-parametric approach was implemented to further explore the association between LV_{GP} and HLM(α), while controlling for multiple comparisons over all time and frequency points of interest. We therefore conducted a cluster-based permutation test using dependent samples regression *t*-statistic to evaluate the effect (linear association) at the sample level. A *p*-value of .05 was chosen for thresholding of the *t*-statistic of the permutation distribution and a critical value corresponding to alpha = .025 (two tailed) was considered for the cluster-level regression test statistic. As depicted in Figure 5, we observed a significant cluster ($p = .005$) extending for the entire 750 ms window of interest (i.e., when covert attention was deployed to the cued stimulus before the contrast changed), which denotes a positive linear association (positive *t*-value) between GP asymmetry and hemispheric lateralized modulation of power centred in the alpha band.

Hemisphere specific relations between alpha modulation and GP asymmetry.

To further investigate the hemisphere-specific influence of GP volumetric asymmetry on alpha modulation indices, we sought to compare MI(α)s of participants according to the directionality of GP lateralization, namely right vs left lateralized GP (see *Materials and Methods*). To this end, we conducted a cluster-based permutation test to compare the groups by means of independent sample t statistic. Analogous to the approach previously described, a *p*-value of .05 was selected as threshold of the *t*-statistic of the permutation distribution and a critical value corresponding to alpha = .025 (two tailed) was considered for the cluster-level independent t-statistic. As visible in Figure 1S, the test indicated a significant cluster of sensors over right posterior channels (p= .027), denoting a difference in right hemisphere MI(α) between the two subgroups. A topographical representation of MI(α) values together with a bar plot of MI(α) averaged across right and left hemisphere ROIs per each group is shown in Figure 2S. Consistently with the GLM results, participants with a bigger right than left GP, also displayed a higher modulation of alpha band, with the cluster based permutation results suggesting that the linear association arising from the GLM was largely driven by a difference in right hemisphere modulation.

Relationship between behavioural measures and globus pallidus asymmetry

With the aim of determining whether GP volumetric asymmetry exerted an influence on task performance, we computed measures of behavioural asymmetry (BA) in accuracy (BA_{ACC}) and reaction times (BA_{RT}) (see Eq.(4), *Materials and Methods*). As for HLM(α), we created an asymmetry index by contrasting behavioural measures for *attend right* with *attend left* trials, holding a positive BA_{RT} value if RTs were faster when validly cued to the left compared to the right, and vice versa. Analogously, positive BA_{ACC} indices reflected higher accuracy in *attend* right trials, compared to *attend* left, and vice versa. Neither behavioural

188 performance asymmetries significantly correlated with LV_{GP} (BA_{RT}: $r = -.12$, $p = .564$;
189 BA_{ACC}: $r = -.06$, $p = .768$) nor HLM(α) (BA_{RT}: $r = -.29$, $p = .155$; BA_{ACC}: $r = .04$, $p = .821$),
190 when averaging across conditions.
191
192 *Association between globus pallidus asymmetry and hemispheric lateralized modulation of*
193 *alpha power as a function of value occurrences*
194 Crucially, we aimed at assessing whether the level of value-salience mediated the association
195 between the derived structural and functional lateralization indices. We first calculated
196 HLM(α) values for each participant, separately for the three value-salience occurrences
197 levels (see *Materials and Methods*), and plotted Pearson correlations with LV_{GP} in the three
198 conditions considered. LV_{GP} significantly correlated with HLM(α) only in trials where both
199 target and distractors were salient (i.e., associated with either positive or negative value) ($r =$
200 $.68$, $p = .000$; Figure 6A). This denotes that, in trials with two items of value-salience,
201 participants exhibiting a right lateralized GP volume, also displayed a stronger alpha
202 modulation in the right compared to the left hemisphere, and vice versa. LV_{GP} did not
203 significantly correlate with HLM(α) when only one or none of the stimuli presented were
204 associated with a salient value ($p = .144$ and $p = .314$, respectively; Figure 6A).
205 In order to statistically quantify the influence of the stimulus-value association on the
206 relationship between LV_{GP} and HLM(α), we compared *robust correlations* in the three
207 conditions according to the method described in [38] for dependent overlapping correlations
208 (see *Materials and Methods*). The correlation between LV_{GP} and HLM(α) in trials with two
209 occurrences of value-salience, significantly differed both from the condition characterized by
210 one (95% CI [.106, .672]) and no occurrences (95% CI [.125, .897]). This confirmed that the
211 association between lateralized GP volume and alpha modulation bias significantly increased
212 as a function of the number of saliency occurrences in the task (Figure 6B).

Discussion

The aim of this study was to uncover the involvement of subcortical structures in modulating spatial attention to stimuli associated with contextual salience. In particular, we investigated the basal ganglia (BG) circuitry in relation to alpha oscillations modulated by attentional allocation [39,40] to items paired with stimulus-value association.

We utilized data in which a modulation of alpha activity by both spatial attention and value-salience associations was established [11]. Next, we observed that BG volumetric asymmetry explained individual differences in hemispheric lateralized modulation (HLM(α)) of absolute alpha power during covert attention. Importantly, this relationship was driven mainly by the Globus Pallidus (GP): participants exhibiting a right lateralized GP also displayed stronger modulation of posterior alpha oscillations in the right hemisphere, and vice versa. The cluster based permutation results confirmed that the association between the structural and functional indices examined was circumscribed to the alpha frequency band, thus underlying selective attentional allocation during the task. Interestingly, this association was largely related to right hemisphere differences in absolute alpha modulation between subjects exhibiting a right as compared to left lateralized GP volume. The latter finding possibly reflects and is explained by the right hemisphere dominance thought to characterize spatial attention processes[41]. Furthermore, we demonstrated that the association between GP asymmetry and alpha hemispheric lateralized modulation (HLM(α)) increased as a function of the saliency occurrences in the task: the correlation between the two indices was significantly higher in trials where both target and distractor were paired with a salient item (reward or loss) as compared to one or zero stimulus pairings. To the best of our knowledge, this is the first finding relating individual differences in BG volumetric lateralization to

interhemispheric modulation of posterior alpha oscillations. Importantly, our results point toward a specific role of GP asymmetry in driving this association.

Our first finding is in line with a growing body of literature demonstrating a subcortical involvement in high level cognitive functions, such as conscious perception [42], working memory performance [43], cognitive control [44–46] and attentional control [47,48]. In line with the latter, we showed that BG volumetric asymmetry predicts individual's biases in the ability to efficiently allocate attention towards the target, as indexed by interhemispheric modulation of alpha power. This is strong evidence in favour of a subcortical involvement in attentional processing, given the well-established role of neuronal synchronization in the alpha band into the selective gating of relevant information during visuospatial covert attention tasks [49,50].

Interestingly, our results emphasize the specific contribution of the GP in implementing stimulus-driven allocation of attention in a value-based context. The GP is considered to mediate the output of the BG. Previous literature has mostly described this structure as primarily involved in voluntary movement regulation: its functions have been indeed predominantly investigated in clinical and animal models in association with motor functions and action control [2,3], describing, for example, reduction of hypokinetic and rigidity symptoms following pallidotomy in humans [51,52] and abnormal pallidal activity in monkeys with induced parkinsonism[3]. Nevertheless, recent results from single unit recordings in humans have provided indications that electrophysiological activity in the globus pallidus pars interna (GPi) reflects processing of stimuli associated with different reward contingencies [53]. This is corroborated by evidence of alterations of cognitive, in addition to motor, abilities, following pallidotomy in Parkinson's disease patients [54]. This aspect has been further addressed in clinical studies showing a link between Parkinson's disease, associated with abnormal pallidal activity [52,55], and altered reward processing as

262 well as updating [56,57]. Structural GP abnormalities have also been linked to psychotic
263 symptoms in schizophrenia [19,21,58], which has been related to aberrant salience attribution
264 and reward learning [22,59], and impaired suppression of distractors in ADHD [16,60].
265 Altogether, these findings point towards the delineation of reinforcement learning networks
266 involving the pallidal complex as the output nucleus within the basal ganglia. Importantly,
267 the correlation between GP asymmetry and HLM(α), particularly arising in trials exhibiting
268 two value-related stimuli, appears to indicate a pallidal engagement during value-driven
269 attentional selection in conflict. The perceptual competition resulting from attending to a
270 salient target whilst required to suppress an equally salient distractor, might be resolved via
271 activity in neural systems involving the GP. Increased midbrain activity has indeed been
272 shown to accompany attentional suppression of a highly rewarding distractor carrying a
273 strong perceptual competition with the target [61], suggesting that dopaminergic networks
274 might flexibly modulate attentional selection in reward-related context. As an important
275 output component of the reward circuit [62], the GP might serve to indirectly modulate the
276 cortical information flow by biasing selective processing of value-related stimuli. While a
277 vast body of literature in the domain of visuospatial attention has investigated cortico-cortical
278 interactions, few studies have focused on elucidating the mechanisms through which cortico-
279 subcortical interactions influence attentional processing. In particular, a dorsal fronto-parietal
280 network has been identified, with nodes around the intraparietal sulcus (IPS) and frontal eye-
281 field (FEF), responsible for mediating top-down allocation of attention. Supporting this
282 notion, both the IPS and FEF have been causally implicated in the control over posterior
283 alpha oscillations in relation to attentional shifts [29–31,40,63]. Yet, recent converging
284 evidence has suggested that BG-cortical interactions play a fundamental role in shaping
285 cognitive processing: in particular, they have been hypothesized to influence frontoparietal

activity during selective attention, by providing signals related to stimulus properties [25,42,64,65].

A subcortical engagement over the modulation of prefrontal activity is exerted via a feedback loop passing through the GP [66–68]. This organization implies a crucial role of the prefrontal cortex in biasing the competition among posterior regions, under the influence of salience driven signals from subcortical sites. The hypothesis of a cortico-BG loop involved in stimulus driven reorienting of attention has been already presented [12,69], conforming to the notion of a 'salience network', which integrates behaviourally relevant input in order to bias and guide cognitive control [70–72]. Within this framework, the BG are thought to influence the connectivity between frontoparietal regions by updating goal-directed behaviour, in order to adapt to changes in the environment [73]. Another intriguing possibility is that signals from the pallidum indirectly influence posterior cortical activity via the thalamus, given its projections to several nuclei of the thalamus, such as the lateral geniculate nucleus (LGN) , reticular nucleus (TRN) [74,75] and the pulvinar [65,76–78], which indirectly connect the GP to cortical sites. The latter was first shown to contribute to the generation of the posterior alpha rhythm in dogs [79] and also to regulate synchronized activity between visual cortical areas to support the allocation of attention in human and nonhuman primates [80–83]. Furthermore, evidence from animal studies describes major connections from the GPi to the lateral habenula, a nucleus located above the thalamus, specifically related to the processing of reward-related stimuli and stimulus-value encoding [84–87].

Therefore, the BG-thalamus loop might exercise its influence by applying control over activity in the prefrontal cortex or it might directly coordinate posterior regions (as reflected by its relationship to alpha power modulation during reward processing). Altogether, these models provide a theoretical framework in favour of a flexible subcortical modulation of top-

311 down regulation of attentional allocation, which appears to be specifically engaged in tasks
312 involving value processing. Nevertheless, the aforementioned possible modulatory routes
313 should not be considered as mutually exclusive: a more comprehensive model of attentional
314 control should account for multiple cortical and subcortical pathways operating in parallel,
315 which would allow optimization of the organism's interaction with the environment.
316 A well-recognized function of the BG is to inhibit or promote cortical activity via
317 GABAergic signalling, through its output in the GP to the thalamus [88,89]. Our results
318 suggest that individual differences in GP volume lateralization may correspond to
319 interhemispheric variability in GABAergic signalling and therefore in the subcortical
320 inhibitory potential to the cortex. This input is likely responsible for producing the
321 mechanisms of 'pulsed inhibition' in the visual cortex [49], reflected by interhemispheric
322 modulation of alpha power, allowing the selective processing of stimuli. Implicitly, we
323 assumed that the volume of the GP indirectly reflects its ability to exert its top-down control
324 over posterior areas, its size possibly representing a determinant for the number of
325 GABAergic neurons involved in the control mechanism.
326 The specificity of the interpretation of our is limited by the difficulty of the segmentation
327 method implemented in distinguishing the contribution of the internal and external parts of
328 the GP, as well as of the delineation of the different thalamic nuclei.
329 In conclusion, our results offer new insight on the mechanisms by which subcortical regions
330 might interact with cortical networks to gate relevant information. In particular, we have
331 provided novel evidence favouring a role for the globus pallidus in providing signals related
332 to the processing of stimulus-value associations, hence influencing posterior alpha
333 oscillations during selective attention to value-salient items.

Materials and Methods

Participants

In the present study, we re-analysed the previously acquired dataset described in [36], where twenty-eight healthy volunteers participated in the study (mean age: 23±2.7 years; 17 female; all right handed). All participant reported normal or corrected-to-normal vision and no prior knowledge of Chinese language. Of these, datasets from three participants were excluded from the analysis (due to respectively: technical error during acquisition, excessive eye movements during MEG recording and structural MRI data not acquired), leaving 25 participants. The experiment was conducted in compliance with the Declaration of Helsinki and was approved by the local ethics board (CMO region Arnhem-Nijmegen, CMO2001/095).

Experimental procedure

The experiment consisted of two phases: in the learning phase, participants were trained to memorize associations between 6 Chinese characters and 3 different values (positive, negative, neutral). Conditioning was implemented by means of visual and auditory feedback: two symbols were associated with reward (+80 cents and a 'kaching' sound), two with loss (-80 cents and a 'buzz' sound) and two with no value (0 cents and a 'beep' sound) (see Figure 1A for an example stimulus-reward association). The stimulus-reward pairing was randomized across participants. Each trial started with the display of three fixation crosses (1000ms), followed by the presentation of a Chinese character (1000ms), together with its matching visual and auditory feedback (Figure 1B). Stimuli were displayed on a grey background, each of them was presented twelve times in a randomized order. The learning phase was conducted in a laboratory with attenuated sound and light and without MEG

359 recording. With the aim of reducing extinction, upon completion of this phase participants
360 were informed that the learnt stimulus-feedback associations would be signalling real reward
361 outcomes throughout the testing phase (i.e. the presentation of a Chinese character,
362 irrespective of its role as target or distractor, would result in a financial reward, loss or none).
363 After the learning phase, participants performed a testing phase (Figure 1C), when they were
364 required to perform a covert spatial attention tasks including the stimuli previously associated
365 with a monetary outcome, while ongoing electromagnetic activity was recorded with MEG.
366 In the testing phase, participants performed 8 blocks of 72 trials. Each trial started with the
367 presentation of three fixation crosses for 1000 ms (pre-trial interval), whose contrast
368 subsequently decreased, as a preparatory cue indicating imminent stimuli presentation. After
369 500ms, two symbols were presented to the left and right of the screen (8 degrees visual angle)
370 respectively, together with a central fixation cross flanked by two arrows, indicating the
371 target side. Participants were instructed to covertly attend the symbol on the cued side
372 ('target') and to ignore the other one ('distractor'), until one of them changed contrast. The
373 contrast change either increased or decreased with equal probability, with onset after 750 ms
374 (13% trials), 1450 ms (47% trials, 'short interval trials') or 2350 ms (40%, 'long interval
375 trials') from stimulus presentation. Participants were asked to report the direction of the
376 contrast change at the targeted ('cued') location as quickly as possible by button press, using
377 the index or middle finger of the right hand to indicate their choice (finger-direction mapping
378 was randomized across participants). Participants were instructed to refrain from responding
379 when the distractor changed contrast. Shorter intervals of 750 ms were used to ensure that
380 participants would start covertly directing their attention rapidly after the cue; these trials
381 were not included in the analysis. The target changed contrast on 95% of the trials (valid
382 trials), whereas in the remaining trials the distractor did (invalid trials). The approximate
383 duration of the full task in the MEG was 50 minutes.

As a result of the conditioning manipulation in the learning phase, targets and distractors in the task would be associated with either a salient (positive or negative) or a neutral value, resulting in three categories of trials of interest, as represented by different levels of value-salience, namely: zero (target and distractor neutral), one (target or distractor salient) or two (target and distractor salient) value-salience levels.

MEG data acquisition

Electromagnetic brain activity was recorded from participants while seated, using a CTF 275-channels whole-head MEG system with axial gradiometers (CTF MEG Systems, VSM MedTech Ltd.). The data were sampled at 1200Hz, following an antialiasing filter set at 300Hz. Head position was constantly monitored throughout the experiment via online head-localization software. This had access to the position of the three head localization coils placed at anatomical fiducials (nasion, left and right ear), allowing, if necessary, readjustment of the participant's position between blocks [90]. Horizontal and vertical EOG and ECG electrodes were recorded with bipolar Ag/AgCl electrodes.

MEG data analysis

MEG data analysis was performed using the FieldTrip Toolbox running in MATLAB [91]. Continuous data were segmented in epochs, centred at the onset of the target contrast change, encompassing the preceding 1500 ms and the following 200 ms (this way covering the full stimulus presentation window for short trials). A notch filter was applied at 50, 100, 150 Hz to remove line noise, the mean was subtracted and the linear trend removed. Automatic artifact rejection was implemented for detection and removal of trials containing eye blinks and horizontal eye movements (detected with EOG), MEG sensor jumps and muscle artifacts. We produced virtual planar gradiometers by computing spatial derivatives of the magnetic

signal recorded with axial gradiometers [92]. The method has the advantage of improving the interpretation of the topographic mapping since neural sources would produce a gradient field directly above them. Time-frequency representations (TFR) of power were then calculated for the resulting pairs of orthogonal planar gradiometers, before summing the power values at each sensor. The analysis was performed by sliding a fixed time window of 500 ms in steps of 50 ms. The resulting data segments were multiplied by a Hanning taper and a fast Fourier transform was applied in the 2 – 30Hz frequency range, in steps of 2Hz. This procedure was applied only for correct valid trials, separately for left and right cued conditions.

For each participant, TFRs were averaged across trials and a Modulation Index (MI) was computed for each sensor *k*, according to the formula:

$$\boldsymbol{MI(f)_k = \frac{Power\ (f)_{k_{att\ right}} - Power\ (f)_{k_{att\ left}}}{Power\ (f)_{k_{att\ right}} + Power\ (f)_{k_{att\ left}}}} \quad \textbf{(1)}$$

Where $Power(f)_{k_{att\ left}}$ represents the power at a given frequency *f* in the condition 'attend left' and $Power\ (f)_{k_{att\ right}}$ is the power of the same frequency in the condition 'attend right'. As a result, positive (or negative) MI values, at a given sensor *k*, indicate higher power at a given frequency when attention was covertly directed towards the right (or left) hemifield.

Two clusters of sensors were then derived, by selecting the twenty symmetrical occipito-parietal sensors (i.e. pairs of ten) showing highest interhemispheric difference in alpha modulation indices, when considering the grand average over all conditions (see Figure 2A). These clusters constituted the regions of interests (ROIs) on which subsequent analysis was focused. Subsequently we calculated the Hemispheric Lateralized Modulation (HLM) index per participant:

$$\boldsymbol{HLM}(\alpha) = \frac{\mathbf{1}}{\boldsymbol{n_{left}}} \sum_{k_{right}=1}^{n_{right}} \boldsymbol{MI}(\alpha)_{k_{right}} + \frac{\mathbf{1}}{\boldsymbol{n_{right}}} \sum_{k_{left}=1}^{n_{left}} \boldsymbol{MI}(\alpha)_{k_{left}} \qquad \textbf{(2)}$$

Where $\boldsymbol{k_{left}}$ and $\boldsymbol{k_{right}}$ denote sensors belonging to the aforementioned left and right clusters, respectively. Since MI(α) values were obtained by subtracting alpha power in 'attend left' trials to 'attend right' trials, and given that alpha power is suppressed in the hemisphere contralateral to the attended hemifield, a positive HLM(α) value indicated that a given participant displayed higher modulation of absolute magnitude of alpha power in the right compared to the left hemisphere, and vice versa (see Figure 2B).

Structural data acquisition

T1-weighted images of three out of twenty five participants were acquired on a 3 T MRI scanner (Magnetom TIM Trio, Siemens Healthcare, Erlangen, Germany), acquisition parameters: TR/TE= 2300/3.03 ms; FA=8°; FoV= 256 × 256 mm; slice thickness= 1 mm; Acquisition matrix= 0×256×256×0. For the remaining participants, a 1.5T MRI scanner was used (Magnetom AVANTO, Siemens Healthcare, Erlangen, Germany). Acquisition parameters: TR/TE= 2250/2.95 ms; FA=15°; FoV= 256 × 256 mm; slice thickness= 1 mm; Acquisition matrix= 0×256×256×0.

Analysis

Structural analyses were conducted using the Integrated Registration and Segmentation Tool (FIRST) within FMRIB's Software Library (FSL) v5.0.9 (www.fmrib.ox.ac.uk/fsl/, Oxford Centre for Functional MRI of the Brain, Oxford, UK). A standard 12 degrees of freedom affine registration to MNI152 space was applied to individual T1 images, adjusted with optimal sub-cortical weighting. Bayesian models implemented in the software are derived

451 from a training based on previous manual segmentation of 336 datasets (provided by the
452 Center for Morphometric Analysis (CMA, MGH, Boston) and applied to registered images to
453 extract subcortical volumetric outputs for left and right hemispheres (see Figure 3A).
454 Given the reward components of the task we then focused on regions of the basal ganglia
455 identified by the algorithm namely the Globus Pallidus (GP), Nucleus Accumbens (NA),
456 Caudate (C) and Putamen (P). To compute hemispheric Lateralized Volume indices (*LV*) for
457 each substructure of interest *s*, we used the following formula, which controls for individual
458 differences in specific subcortical volumes via normalization by total bilateral volume,
459 commonly employed to evaluate structural brain asymmetries [22,93]:

$$\boldsymbol{LV(s)} = \frac{\boldsymbol{V(s)_{right}} - \boldsymbol{V(s)_{left}}}{\boldsymbol{V(s)_{right}} + \boldsymbol{V(s)_{left}}} \quad \textbf{(3)}$$

460 Where $\boldsymbol{V_{S_{right}}}$ and $\boldsymbol{V_{S_{left}}}$ represent respectively the anatomical right and left volumes (in
461 voxels) for a given substructure *s*. Analogously to equation(2), a positive (or negative) LV_S
462 index, in a given participant, indicated a greater right (or left) volume for a given substructure
463 *s* (see Figure 3B).
464
465 *Behavioural data analysis*
466 To investigate the possible association of behavioural performance with structural and
467 functional hemispheric lateralization, we correlated individual asymmetries in accuracy
468 (ACC) (percentage of correct responses) and reaction times (RTs) with individual HLM(α)
469 and LV values of subcortical structures showing significant correlation with HLM(α). For
470 each subject, behavioural asymmetries in performance (BA) for both measures were
471 calculated according to:

$$\boldsymbol{BA_{RT/ACC}} = \frac{\boldsymbol{BA_{RT/ACC_{right}}} - \boldsymbol{BA_{RT/ACC_{left}}}}{\boldsymbol{BA_{RT/ACC_{right}}} + \boldsymbol{BA_{RT/ACC_{left}}}} \quad \textbf{(4)}$$

Where $BA_{RT\ right}$ and $BA_{RT\ left}$ represent mean reaction times for 'attend right' and 'attend left' trials, respectively. A positive BA_{RT} for a given subject indicated faster responses when a participant was validly cued to the left compared to the right hemisphere, while negative values indicated the opposite pattern. Consequently, positive BA_{ACC} values indicated higher accuracy on 'attend right' trials compared to 'left attend' trials, and vice versa.

Statistics

Generalized Linear Model

In order to determine the relationship between Basal Ganglia Lateralized Volumes (LV_S) and electromagnetic indices (HLM(α)) we applied a generalized linear regression model (GLM), specifying subcortical volumes lateralization (*LV* values) as regressors and individual HLM values as the response vector, according to the formula:

$$\boldsymbol{HLM}(\alpha) \sim \boldsymbol{\beta_0} + \boldsymbol{\beta_1 LV_{GP}} + \boldsymbol{\beta_2 LV_{NAcc}} + \boldsymbol{\beta_3 LV_{CN}} + \boldsymbol{\beta_4 LV_{Pu}} + \boldsymbol{\varepsilon} \quad \textbf{(5)}$$

All subsequent analysis on the relationship between volumetric and oscillatory data specifically focused only on the subcortical structure(s) associated with a significant β coefficient in the model in equation(5).

487 *Cluster based permutation test*

488 To evaluate whether the linear association between LV_s and HLM was effectively limited to
489 the alpha band, a cluster based permutation approach [94] was employed over the full time
490 frequency spectrum of interest. This method effectively allows to statistically control for
491 multiple comparisons over all time and frequency points of interest. After selecting the a-
492 priori sensors belonging to the formerly specified ROIs, we considered a permutation
493 distribution of regression coefficients derived from randomly pairing participants' LV_s value
494 (independent variable) and modulation indices (HLM(*f*)) 1000 times. At every time-by-
495 frequency point, the actual regression coefficient was evaluated against the aforementioned
496 distribution by means of a specified critical α value. Afterwards, a time-frequency map of the
497 cluster level statistics was derived showing sets of sensors associated with a significant
498 effect.

499 An equivalent approach was later applied to investigate possible hemisphere-specific
500 differences in alpha modulation between participants showing a right or left lateralized
501 substructure s. Directionality of lateralization was determined by median split of the
502 distribution of LV_s per participant, producing two subgroups of N=12, representing subjects
503 with a larger left or right volume of substructure s. After having a-priori averaged across the
504 time-frequency spectrum of interest ([-750 0]ms, 8-13Hz), MI(α) values at every sensor were
505 compared between the two subgroups (right vs left lateralized substructure). The actual t-
506 value was then compared with a permutation distribution of t-statistic derived from randomly
507 partitioning indices between the two groups 1000 times. As a result, a topography map was
508 plotted displaying eventual cluster(s) of sensors associated with a significant t-value (i.e. a
509 significant difference in MI(α) between subgroups).

510

511

Comparison between Pearson's correlation coefficients

Finally, we aimed at comparing the association between the derived structural and functional lateralization indices in different reward-related contingencies. To this end, we calculated HLM(α) values for each participant separately for the three reward-related contingencies and computed the Pearson's correlations with LV_S indices. We statistically assessed the difference in correlation coefficients between the three experimental conditions considered, according to the method described in [95]. The test implements a percentile resampling technique by generating a bootstrap sample of the difference of the correlation coefficients between the overlapping variable LV_{GP} (Y) and the two variables representing the HLM(α) for the two experimental conditions (reward contingencies) to be compared (X_1, X_2). As suggested in the method, we used a Winsorized correlation to achieve a robust measure of association between variables. This transformation has been shown to effectively control for the influence of outliers on the correlation estimate [96]. A confidence interval was then computed on the resulting bootstrap distribution, to assess the statistical significance of the actual difference between correlation coefficients describing the different value occurrences.

Data availability

The preprocessed MEG and MRI anonymised datasets that support the findings of this study are available as downloadable online data collection in the Donders Data Repository (https://data.donders.ru.nl), with persistent identifier: 11633/di.dccn.DSC_3016045.01_337, upon reasonable request to the corresponding author.

Acknowledgements

The authors gratefully acknowledge the support of the Netherlands Organisation for Scientific Research (NWO, VICI grants 453-09-002 and 453-14-015 and the James S.

McDonnell Foundation (grants 220020328 and 220020448). We also would like to thank Sebastiaan den Boer for his in contribution in the data collection process and experimental design.

References

1. Groenewegen HJ. The Basal Ganglia and Motor Control. Neural Plast. 2003;10: 107–120. doi:10.1155/NP.2003.107

2. Jahfari S, Waldorp L, van den Wildenberg WPM, Scholte HS, Ridderinkhof KR, Forstmann BU. Effective Connectivity Reveals Important Roles for Both the Hyperdirect (Fronto-Subthalamic) and the Indirect (Fronto-Striatal-Pallidal) Fronto-Basal Ganglia Pathways during Response Inhibition. J Neurosci. 2011;31: 6891–6899. doi:10.1523/JNEUROSCI.5253-10.2011

3. Filion M, Tremblay L. Abnormal spontaneous activity of globus pallidus neurons in monkeys with MPTP-induced parkinsonism. Brain Res. 1991;547: 140–144. doi:10.1016/0006-8993(91)90585-J

4. Mehler-Wex C, Riederer P, Gerlach M. Dopaminergic dysbalance in distinct basal ganglia neurocircuits: Implications for the pathophysiology of parkinson's disease, schizophrenia and attention deficit hyperactivity disorder. Neurotox Res. 2006;10: 167–179. doi:10.1007/BF03033354

5. Schechtman E, Noblejas MI, Mizrahi AD, Dauber O, Bergman H. Pallidal spiking activity reflects learning dynamics and predicts performance. Proc Natl Acad Sci. 2016;113: E6281–E6289. doi:10.1073/pnas.1612392113

6. Lauwereyns J, Takikawa Y, Kawagoe R, Kobayashi S, Koizumi M, Coe B, et al. Feature-based anticipation of cues that predict reward in monkey caudate nucleus. Neuron. 2002;33: 463–473. doi:10.1016/S0896-6273(02)00571-8

7. Schultz W, Tremblay L, Hollerman JR, Schultz. Reward processing in primate orbitofrontal cortex and basal ganglia. Cereb Cortex. 2000;10: 272–284. doi:10.1093/cercor/10.3.272

564 8. Tremblay L, Hollerman JR, Schultz W. Modifications of reward expectation-related
565 neuronal activity during learning in primate striatum. J Neurophysiol. 1998;80: 964–
566 977.

567 9. van Schouwenburg M, Aarts E, Cools R. Dopaminergic modulation of cognitive
568 control: distinct roles for the prefrontal cortex and the basal ganglia. Curr Pharm Des.
569 2010;16: 2026–2032. doi:10.2174/138161210791293097

570 10. Van Schouwenburg MR, Den Ouden HEM, Cools R. Selective attentional
571 enhancement and inhibition of fronto-posterior connectivity by the basal ganglia
572 during attention switching. Cereb Cortex. 2015;25: 1527–1534.
573 doi:10.1093/cercor/bht345

574 11. Tommasi G, Fiorio M, Yelnik J, Krack P, Sala F, Schmitt E, et al. Disentangling the
575 Role of Cortico-Basal Ganglia Loops in Top–Down and Bottom–Up Visual Attention:
576 An Investigation of Attention Deficits in Parkinson Disease. J Cogn Neurosci. MIT
577 Press; 2014;27: 1215–1237. doi:10.1162/jocn_a_00770

578 12. Shulman GL, Astafiev S V, Franke D, Pope DLW, Abraham Z, Mcavoy MP, et al.
579 Interaction of stimulus-driven reorienting and expectation in ventral and dorsal fronto-
580 parietal and basal ganglia-cortical networks. 2010;29: 4392–4407.
581 doi:10.1523/JNEUROSCI.5609-08.2009.Interaction

582 13. Braunlich K, Seger C. The basal ganglia. Wiley Interdiscip Rev Cogn Sci. 2013;4:
583 135–148. doi:10.1002/wcs.1217

584 14. Hikosaka O, Bromberg-Martin E, Hong S, Matsumoto M. New insights on the
585 subcortical representation of reward. Curr Opin Neurobiol. 2008;18: 203–208.
586 doi:10.1016/j.conb.2008.07.002

587 15. Hikosaka O, Kim HF, Yasuda M, Yamamoto S. Basal Ganglia Circuits for Reward

Value–Guided Behavior. Annu Rev Neurosci. 2014;37: 289–306. doi:10.1146/annurev-neuro-071013-013924

16. Aylward EH, Reiss AL, Reader MJ, Singer HS, Brown JE, Denckla MB. Basal ganglia volumes in children with attention-deficit hyperactivity disorder. J Child Neurol. 1996;11: 112–115. doi:10.1177/088307389601100210

17. Qui A, Crocetti D, Adler M, Mahone EM, Denckla MB, Miller MI, et al. Basal ganglia volume and shape in children with attention deficit hyperactivity disorder. Am J Psychiatry. 2009;166: 74–82. doi:10.1176/appi.ajp.2008.08030426.Basal

18. Paclt I, Přibilová N, Kollárová P, Kohoutová M, Dezortová M, Hájek M, et al. Reverse asymmetry and changes in brain structural volume of the basal ganglia in ADHD, developmental changes and the impact of stimulant medications. Neuroendocrinol Lett. 2016;37: 29–32.

19. Hokama H, Shenton ME, Nestor PG, Kikinis R, Levitt JJ, Metcalf D, et al. Caudate, putamen, and globus pallidus volume in schizophrenia: A quantitative MRI study. Psychiatry Res Neuroimaging. 1995;61: 209–229. doi:10.1016/0925-4927(95)02729-H

20. Womer FY, Wang L, Alpert KI, Smith MJ, Csernansky JG, Barch DM, et al. Basal ganglia and thalamic morphology in schizophrenia and bipolar disorder. Psychiatry Res - Neuroimaging. Elsevier; 2014;223: 75–83. doi:10.1016/j.pscychresns.2014.05.017

21. Mamah D, Wang L, Barch D, de Erausquin GA, Gado M, Csernansky JG. Structural analysis of the basal ganglia in schizophrenia. Schizophr Res. 2007;89: 59–71. doi:10.1016/j.schres.2006.08.031

22. Okada N, Fukunaga M, Yamashita F, Koshiyama D, Yamamori H, Ohi K, et al.

612 Abnormal asymmetries in subcortical brain volume in schizophrenia. Mol Psychiatry.
613 Nature Publishing Group; 2016;21: 1–7. doi:10.1038/mp.2015.209

614 23. Howes OD, Nour MM. Dopamine and the aberrant salience hypothesis of
615 schizophrenia. World Psychiatry. 2016;15: 3–4. doi:10.1002/wps.20276

616 24. Nobre, K., & Kastner S. The Oxford handbook of attention. Oxford: Oxford University
617 Press; 2014.

618 25. Chelazzi L, Perlato A, Santandrea E, Della Libera C. Rewards teach visual selective
619 attention. Vision Res. Elsevier Ltd; 2013;85: 58–62. doi:10.1016/j.visres.2012.12.005

620 26. Thut G. -Band Electroencephalographic Activity over Occipital Cortex Indexes
621 Visuospatial Attention Bias and Predicts Visual Target Detection. J Neurosci. 2006;26:
622 9494–9502. doi:10.1523/JNEUROSCI.0875-06.2006

623 27. Kelly SP. Increases in Alpha Oscillatory Power Reflect an Active Retinotopic
624 Mechanism for Distracter Suppression During Sustained Visuospatial Attention. J
625 Neurophysiol. 2006;95: 3844–3851. doi:10.1152/jn.01234.2005

626 28. Worden MS, Foxe JJ, Wang N, Simpson G V. Anticipatory biasing of visuospatial
627 attention indexed by retinotopically specific alpha-band electroencephalography
628 increases over occipital cortex. J Neurosci. 2000;20: RC63.

629 29. Ptak R. The Frontoparietal Attention Network of the Human Brain. Neurosci. 2012;18:
630 502–515. doi:10.1177/1073858411409051

631 30. Vossel S, Geng JJ, Fink GR. Dorsal and Ventral Attention Systems. Neurosci.
632 2014;20: 150–159. doi:10.1177/1073858413494269

633 31. Marshall TR, Bergmann TO, Jensen O. Frontoparietal Structural Connectivity
634 Mediates the Top-Down Control of Neuronal Synchronization Associated with
635 Selective Attention. PLoS Biol. 2015;13: 1–17. doi:10.1371/journal.pbio.1002272

636 32. Marshall TR, O'Shea J, Jensen O, Bergmann TO. Frontal Eye Fields Control
637 Attentional Modulation of Alpha and Gamma Oscillations in Contralateral
638 Occipitoparietal Cortex. J Neurosci. 2015;35: 1638–1647.
639 doi:10.1523/JNEUROSCI.3116-14.2015

640 33. Capotosto P, Corbetta M, Romani GL, Babiloni C. Electrophysiological correlates of
641 stimulus-driven reorienting deficits after interference with right parietal cortex during
642 a spatial attention task: a TMS-EEG study. J Cogn Neurosci. 2012;24:
643 10.1162/jocn_a_00287. doi:10.1162/jocn_a_00287

644 34. Tomer R, Goldstein RZ, Wang G-J, Wong C, Volkow ND. Incentive motivation is
645 associated with striatal dopamine asymmetry. Biol Psychol. 2008;77: 98–101.
646 doi:10.1016/j.biopsycho.2007.08.001

647 35. Tomer R, Slagter HA, Christian BT, Fox AS, King CR, Murali D, et al. Dopamine
648 Asymmetries Predict Orienting Bias in Healthy Individuals. Cereb Cortex. 2013;23:
649 2899–2904. doi:10.1093/cercor/bhs277

650 36. Marshall TR, den Boer S, Cools R, Jensen O, Fallon SJ, Zumer JM. Occipital Alpha
651 and Gamma Oscillations Support Complementary Mechanisms for Processing
652 Stimulus Value Associations. J Cogn Neurosci. MIT Press; 2017; 1–11.
653 doi:10.1162/jocn_a_01185

654 37. Dillon DG, Holmes AJ, Birk JL, Brooks N, Lyons-Ruth K, Pizzagalli DA. Childhood
655 Adversity Is Associated with Left Basal Ganglia Dysfunction During Reward
656 Anticipation in Adulthood. Biol Psychiatry. Society of Biological Psychiatry; 2009;66:
657 206–213. doi:10.1016/j.biopsych.2009.02.019

658 38. Wilcox RR. Comparing dependent robust correlations. Br J Math Stat Psychol.
659 2016;69: 215–224. doi:10.1111/bmsp.12069

660 39. Marshall TR, O'Shea J, Jensen O, Bergmann TO. Frontal Eye Fields Control
661 Attentional Modulation of Alpha and Gamma Oscillations in Contralateral
662 Occipitoparietal Cortex. J Neurosci. 2015;35: 1638–1647.
663 doi:10.1523/JNEUROSCI.3116-14.2015

664 40. Corbetta M, Shulman GL. Control of Goal-Directed and Stimulus-Driven Attention in
665 the Brain. Nat Rev Neurosci. 2002;3: 215–229. doi:10.1038/nrn755

666 41. Shulman GL, Pope DLW, Astafiev S V., McAvoy MP, Snyder AZ, Corbetta M. Right
667 Hemisphere Dominance during Spatial Selective Attention and Target Detection
668 Occurs Outside the Dorsal Frontoparietal Network. J Neurosci. 2010;30: 3640–3651.
669 doi:10.1523/JNEUROSCI.4085-09.2010

670 42. Slagter HA, Mazaheri A, Reteig LC, Smolders R, Figee M, Mantione M, et al.
671 Contributions of the ventral striatum to conscious perception: An intracranial EEG
672 study of the attentional blink. J Neurosci. 2016;37: 1081–1089.
673 doi:10.1523/JNEUROSCI.2282-16.2016

674 43. Frank MJ, Loughry B, O'Reilly RC. Interactions between frontal cortex and basal
675 ganglia in working memory: A computational model. Cogn Affect Behav Neurosci.
676 2001;1: 137–160. doi:10.3758/CABN.1.2.137

677 44. Reilly RCO, Herd SA, Pauli WM. Computational Models of Cognitive Control.
678 Psychology. 2011;20: 257–261. doi:10.1016/j.conb.2010.01.008.Computational

679 45. Ceaser AE, Barch DM. Striatal Activity is Associated with Deficits of Cognitive
680 Control and Aberrant Salience for Patients with Schizophrenia. Front Hum Neurosci.
681 2015;9: 687. doi:10.3389/fnhum.2015.00687

682 46. Piray P, Toni I, Cools R. Human Choice Strategy Varies with Anatomical Projections
683 from Ventromedial Prefrontal Cortex to Medial Striatum. J Neurosci. 2016;36: 2857–

2867. doi:10.1523/JNEUROSCI.2033-15.2016

47. Yantis S, Anderson BA, Wampler EK, Laurent PA. Reward and attentional control in visual search. Nebr Symp Motiv. 2012;59: 91–116. doi:10.1111/j.1600-6143.2008.02497.x.Plasma

48. Tommasi G, Fiorio M, Yelnik J, Krack P, Sala F, Schmitt E, et al. Disentangling the Role of Cortico-Basal Ganglia Loops in Top–Down and Bottom–Up Visual Attention: An Investigation of Attention Deficits in Parkinson Disease. J Cogn Neurosci. MIT Press; 2015;27: 1215–1237. doi:10.1162/jocn_a_00770

49. Jensen O, Mazaheri A. Shaping functional architecture by oscillatory alpha activity: gating by inhibition. Front Hum Neurosci. 2010;4: 186. doi:10.3389/fnhum.2010.00186

50. Fries P. Modulation of Oscillatory Neuronal Synchronization by Selective Visual Attention. Science (80-). 2001;291: 1560–1563. doi:10.1126/science.1055465

51. Schuurman PR, de Bie RMA, Speelman JD, Bosch DA. Posteroventral Pallidotomy in Movement Disorders. In: Ostertag CB, Thomas DGT, Bosch A, Linderoth B, Broggi G, editors. Advances in Stereotactic and Functional Neurosurgery 12: Proceedings of the 12th Meeting of the European Society for Stereotactic and Functional Neurosurgery, Milan 1996. Vienna: Springer Vienna; 1997. pp. 14–17. doi:10.1007/978-3-7091-6513-3_3

52. Dostrovsky JO, Hutchison WD, Lozano AM. The Globus Pallidus , Deep Brain Stimulation , and Parkinson ' s Disease. Neurosci. 2002;8: 284–290. doi:10.1177/1073858402008003014

53. Howell NA, Prescott IA, Lozano AM, Hodaie M, Voon V, Hutchison WD. Preliminary evidence for human globus pallidus pars interna neurons signaling reward

708 and sensory stimuli. Neuroscience. IBRO; 2016;328: 30–39.
709 doi:10.1016/j.neuroscience.2016.04.020

710 54. Lombardi WJ, Gross RE, Trepanier LL, Lang AE, Lozano AM, Saint-Cyr JA.
711 Relationship of lesion location to cognitive outcome following microelectrode-guided
712 pallidotomy for Parkinson's disease: support for the existence of cognitive circuits in
713 the human pallidum. Brain. 2000;123: 746–758. doi:10.1093/brain/123.4.746

714 55. Rosenberg-Katz K, Herman T, Jacob Y, Kliper E, Giladi N, Hausdorff JM. Subcortical
715 Volumes Differ in Parkinson's Disease Motor Subtypes: New Insights into the
716 Pathophysiology of Disparate Symptoms. Front Hum Neurosci. 2016;10: 1–9.
717 doi:10.3389/fnhum.2016.00356

718 56. Aarts E, Helmich RC, Janssen MJR, Oyen WJG, Bloem BR, Cools R. Aberrant reward
719 processing in Parkinson's disease is associated with dopamine cell loss. Neuroimage.
720 Elsevier Inc.; 2012;59: 3339–3346. doi:10.1016/j.neuroimage.2011.11.073

721 57. Chong TTJ, Bonnelle V, Manohar S, Veromann KR, Muhammed K, Tofaris GK, et al.
722 Dopamine enhances willingness to exert effort for reward in Parkinson's disease.
723 Cortex. Elsevier Ltd; 2015;69: 40–46. doi:10.1016/j.cortex.2015.04.003

724 58. Spinks R, Nopoulos P, Ward J, Fuller R, Magnotta VA, Andreasen NC. Globus
725 pallidus volume is related to symptom severity in neuroleptic naive patients with
726 schizophrenia. Schizophr Res. 2005;73: 229–233. doi:10.1016/j.schres.2004.05.020

727 59. Early TS, Reiman EM, Raichle ME, Spitznagel EL. Left globus pallidus abnormality
728 in never-medicated patients with schizophrenia. Proc Natl Acad Sci U S A. 1987;84:
729 561–563.

730 60. Qiu A, Crocetti D, Adler M, Mahone EM, Denckla MB, Miller MI, et al. Basal ganglia
731 volume and shape in children with attention deficit hyperactivity disorder. Am J

732 Psychiatry. 2009;166: 74–82. doi:10.1176/appi.ajp.2008.08030426

733 61. Gong M, Jia K, Li S. Perceptual Competition Promotes Suppression of Reward
734 Salience in Behavioral Selection and Neural Representation. J Neurosci. 2017;37:
735 6242–6252. doi:10.1523/JNEUROSCI.0217-17.2017

736 62. Haber S. Neuroanatomy of Reward: A View from the Ventral Striatum. In: Jay A.
737 Gottfried, editor. Neurobiology of Sensation and Reward. CRC Press; 2011.
738 doi:10.1201/b10776-15

739 63. Capotosto P, Corbetta M, Romani GL, Babiloni C. Electrophysiological correlates of
740 stimulus-driven reorienting deficits after interference with right parietal cortex during
741 a spatial attention task: a TMS-EEG study. J Cogn Neurosci. 2012;24:
742 10.1162/jocn_a_00287. doi:10.1162/jocn_a_00287

743 64. Overton PG, Vautrelle N, Redgrave P. Sensory regulation of dopaminergic cell
744 activity: Phenomenology, circuitry and function. Neuroscience. IBRO; 2014;282: 1–
745 12. doi:10.1016/j.neuroscience.2014.01.023

746 65. Saalmann YB, Kastner S. Cognitive and Perceptual Functions of the Visual Thalamus.
747 Neuron. Elsevier Inc.; 2011;71: 209–223. doi:10.1016/j.neuron.2011.06.027

748 66. Cummings J. Frontal-subcortical circuits and human behavior. Arch Neurol. 1993;50:
749 873–880. doi:10.1001/archneur.1993.00540080076020

750 67. Pauls DL, Abramovitch A, Rauch SL, Geller DA. Obsessive–compulsive disorder: an
751 integrative genetic and neurobiological perspective. Nat Rev Neurosci. Nature
752 Publishing Group; 2014;15: 410–424. doi:10.1038/nrn3746

753 68. Saunders A, Oldenburg IA, Berezovskii VK, Johnson CA, Kingery ND, Elliott HL, et
754 al. A direct GABAergic output from the basal ganglia to frontal cortex. Nature. Nature
755 Publishing Group, a division of Macmillan Publishers Limited. All Rights Reserved.;

2015;521: 85. doi:10.1038/nature14179

69. Alexander G. Parallel Organization of Functionally Segregated Circuits Linking Basal Ganglia and Cortex. Annu Rev Neurosci. 1986;9: 357–381. doi:10.1146/annurev.neuro.9.1.357

70. Metzger CD. High field fMRI reveals thalamocortical integration of segregated cognitive and emotional processing in mediodorsal and intralaminar thalamic nuclei. Front Neuroanat. 2010;4: 1–17. doi:10.3389/fnana.2010.00138

71. Peters SK, Dunlop K, Downar J. Cortico-Striatal-Thalamic Loop Circuits of the Salience Network: A Central Pathway in Psychiatric Disease and Treatment. Front Syst Neurosci. 2016;10: 1–23. doi:10.3389/fnsys.2016.00104

72. Seeley WW, Menon V, Schatzberg AF, Keller J, Glover GH, Kenna H, et al. Dissociable Intrinsic Connectivity Networks for Salience Processing and Executive Control. J Neurosci. 2007;27: 2349–2356. doi:10.1523/JNEUROSCI.5587-06.2007

73. van Schouwenburg MR, den Ouden HEM, Cools R. The Human Basal Ganglia Modulate Frontal-Posterior Connectivity during Attention Shifting. J Neurosci. 2010;30: 9910–9918. doi:10.1523/JNEUROSCI.1111-10.2010

74. Pazo JH, Barceló AC, Bellantonio E, Pazo VC, Almarares N. Electrophysiologic study of globus pallidus projections to the thalamic reticular nucleus. Brain Res Bull. Elsevier Inc.; 2013;94: 82–89. doi:10.1016/j.brainresbull.2013.02.009

75. Villalobos N, Oviedo-Chávez A, Alatorre A, Ríos A, Barrientos R, Delgado A, et al. Striatum and globus pallidus control the electrical activity of reticular thalamic nuclei. Brain Res. Elsevier; 2016;1644: 258–266. doi:10.1016/j.brainres.2016.05.032

76. Zhou H, Schafer RJ, Desimone R. Pulvinar-Cortex Interactions in Vision and Attention. Neuron. Elsevier Inc.; 2016;89: 209–220. doi:10.1016/j.neuron.2015.11.034

780 77. Laberge D, Buchsbaum MS. Positron Emission Tomographic Measurements of
781 Pulvinar Activity During an Attention Task. J Neurosci. 1990;10: 613–619.

782 78. Shipp S. The brain circuitry of attention. Trends Cogn Sci. 2004;8: 223–230.
783 doi:10.1016/j.tics.2004.03.004

784 79. Lopes da Silva FH, Vos JE, Mooibroek J, van Rotterdam A. Relative contributions of
785 intracortical and thalamo-cortical processes in the generation of alpha rhythms,
786 revealed by partial coherence analysis. Electroencephalogr Clin Neurophysiol.
787 1980;50: 449–456. doi:10.1016/0013-4694(80)90011-5

788 80. Saalmann YB, Pinsk MA, Wang L, Li X, Kastner S. The Pulvinar Regulates
789 Information Transmission Between Cortical Areas Based on Attention Demands.
790 Science (80-). 2012;337: 753–756. doi:10.1126/science.1223082

791 81. Green JJ, Boehler CN, Roberts KC, Chen L-C, Krebs RM, Song AW, et al. Cortical
792 and Subcortical Coordination of Visual Spatial Attention Revealed by Simultaneous
793 EEG–fMRI Recording. J Neurosci. 2017;37: 7803–7810.
794 doi:10.1523/JNEUROSCI.0326-17.2017

795 82. Petersen SE, Robinson DL, Morris JD. Contributions of the pulvinar to visual spatial
796 attention. Neuropsychologia. 1987;25: 97–105. doi:10.1016/0028-3932(87)90046-7

797 83. Kastner S, O'Connor DH, Fukui MM, Fehd HM, Herwig U, Pinsk MA. Functional
798 imaging of the human lateral geniculate nucleus and pulvinar. J Neurophysiol.
799 2004;91: 438–448. doi:10.1152/jn.00553.2003

800 84. Bromberg-Martin ES, Matsumoto M, Hong S, Hikosaka O. A Pallidus-Habenula-
801 Dopamine Pathway Signals Inferred Stimulus Values. J Neurophysiol. 2010;104:
802 1068–1076. doi:10.1152/jn.00158.2010

803 85. Hong S, Hikosaka O. The Globus Pallidus Sends Reward-Related Signals to the

Lateral Habenula. Neuron. Elsevier Inc.; 2008;60: 720–729. doi:10.1016/j.neuron.2008.09.035

86. Matsumoto M, Hikosaka O. Lateral habenula as a source of negative reward signals in dopamine neurons. Nature. 2007;447: 1111–1115. Available: http://dx.doi.org/10.1038/nature05860

87. Baker PM, Jhou T, Li B, Matsumoto M, Mizumori SJY, Stephenson-Jones M, et al. The Lateral Habenula Circuitry: Reward Processing and Cognitive Control. J Neurosci. 2016;36: 11482–11488. doi:10.1523/JNEUROSCI.2350-16.2016

88. Goldberg JH, Farries MA, Fee MS. Basal ganglia output to the thalamus: still a paradox. Trends Neurosci. 2013;36: 10.1016/j.tins.2013.09.001. doi:10.1016/j.tins.2013.09.001

89. Lanciego JL, Luquin N, Obeso JA. Functional neuroanatomy of the basal ganglia. Cold Spring Harb Perspect Med. 2012;2: 1–20. doi:10.1101/cshperspect.a009621

90. Stolk A, Todorovic A, Schoffelen JM, Oostenveld R. Online and offline tools for head movement compensation in MEG. Neuroimage. Elsevier Inc.; 2013;68: 39–48. doi:10.1016/j.neuroimage.2012.11.047

91. Oostenveld R, Fries P, Maris E, Schoffelen JM. FieldTrip: Open source software for advanced analysis of MEG, EEG, and invasive electrophysiological data. Comput Intell Neurosci. 2011;2011. doi:10.1155/2011/156869

92. Bastiaansen MCM, Knösche TR. Tangential derivative mapping of axial MEG applied to event-related desynchronization research. Clin Neurophysiol. 2000;111: 1300–1305. doi:10.1016/S1388-2457(00)00272-8

93. Guadalupe T, Mathias SR, VanErp TGM, Whelan CD, Zwiers MP, Abe Y, et al. Human subcortical brain asymmetries in 15,847 people worldwide reveal effects of

age and sex. Brain Imaging Behav. 2016; 1–18. doi:10.1007/s11682-016-9629-z

94. Maris E, Oostenveld R. Nonparametric statistical testing of EEG- and MEG-data. J Neurosci Methods. 2007;164: 177–190. doi:10.1016/j.jneumeth.2007.03.024

95. Wilcox RR. Comparing dependent robust correlations. Br J Math Stat Psychol. 2016;69: 215–224. doi:10.1111/bmsp.12069

96. Wilcox RR. Introduction to Robust Estimation and Hypothesis Testing. Academic Press; 2016.

97. Bischoff-Grethe A, Ozyurt IB, Busa E, Quinn BT, Fennema-Notestine C, Clark CP, et al. A technique for the deidentification of structural brain MR images. Hum Brain Mapp. 2007;28: 892–903. doi:10.1002/hbm.20312

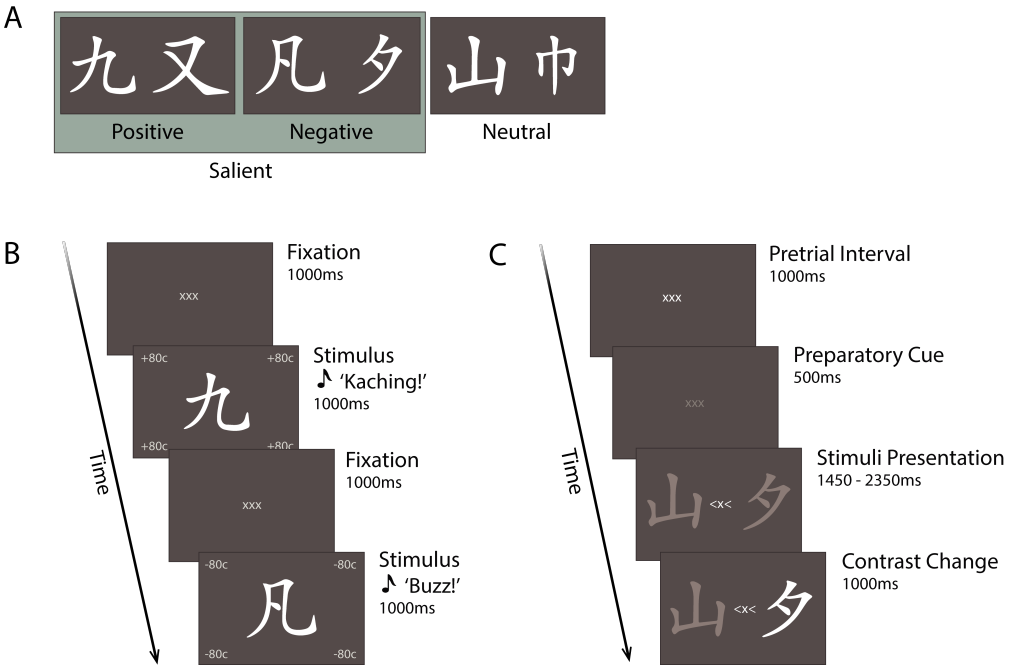

Figure 1. Illustration of selective attention task: stimuli and reward manipulation.

(A) Six Chinese symbols served as stimuli for the task and were associated with three values: two paired with reward, two with loss and two with no financial change (neutral). (B) Representative trial of the learning phase. Symbols were displayed for 1000ms, systematically paired with the corresponding (positive, negative or neutral) value, via visual and auditory feedback. Characters presentation was alternated with a 1000ms fixation period. During the training phase, participants learned associations between the stimuli and their reward value. **C.** Representative trial of the testing phase. After a 1000ms pretrial interval, participants were primed with a 500ms preparatory cue signalling the upcoming stimuli. Two characters were then presented to the left and right hemifield, together with a spatial cue, instructing participants to covertly attend the symbol on the cued side (target) and ignore the other one (distractor). Participants' task was to report when the target stimulus changed contrast. Contrast change could either occur after 750ms (13% of trials), 1450ms (47% of trials) or 2350ms (40% of the trials). In 95% of the trials, the target changed contrast (valid trials), whilst in 5% of the trials, the distractor changed contrast (invalid trials). Figure adapted from [36].

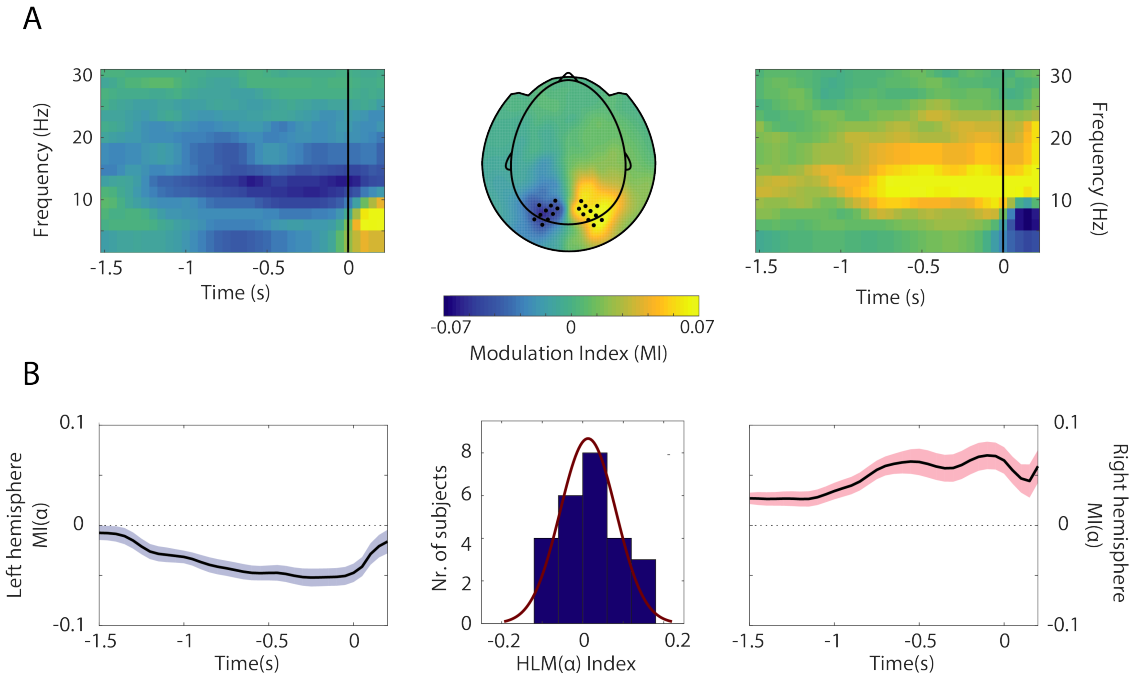

Figure 2. Grand average MI and HLM distribution across participants.

(A) Time-frequency representations of power (TFRs) and topographical plot showing contrast between the 'attention right' – 'attention left' trials. A clear modulation is visible at posterior sensors in the alpha band (8 – 13Hz) and the –750 – 0ms interval. Sensors included in the left and right ROIs are marked as dots. Trials are locked to the onset of the contrast change (t = 0). (B) Side panels show the temporal evolution of MI(α), averaged over sensors within left and right hemisphere ROIs. The magnitude (absolute value) of alpha modulation progressively increased in the stimulus interval until the onset of the contrast change. Middle: distribution of HLM(α) indices across participants, computed over the ROIs and 8 – 13 Hz frequency band (see Materials and Methods). A normal density function is superimposed, denoting no hemispheric bias in lateralized modulation values across participants (Shapiro Wilk, $W = .958$, $p = .392$).

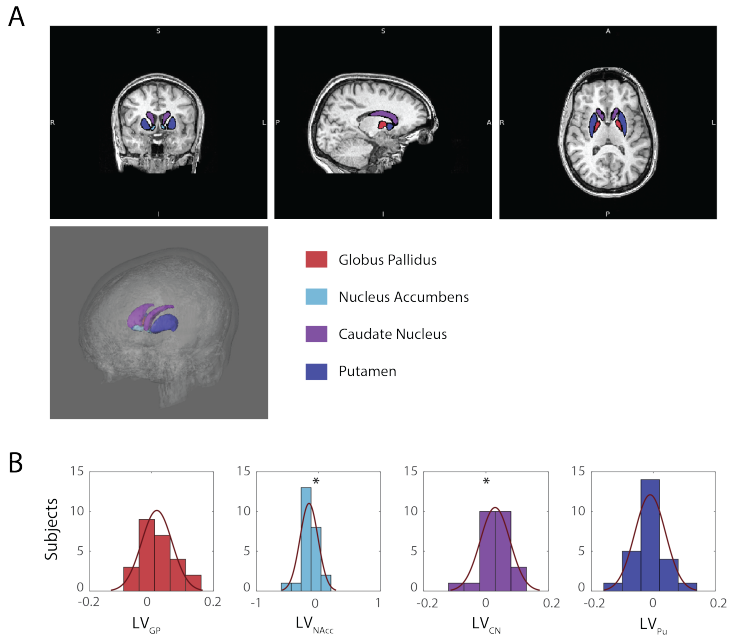

Figure 3. Basal Ganglia volumes resulting from semiautomated subcortical segmentation implemented. (A) Orthogonal view and 3D rendering. Subcortical volumes are overlaid as meshes on the anatomical MRI of one of the participants (following defacing procedure in Freesurfer, where voxels outside the brain mask with identifiable facial features were excluded [97]). (B) Histograms with superimposition of normal density function, showing the distribution of subcortical lateralization indices for each substructure. In our sample, NAcc was right lateralized (p = .0001) and CN was left lateralized (p = .0029).

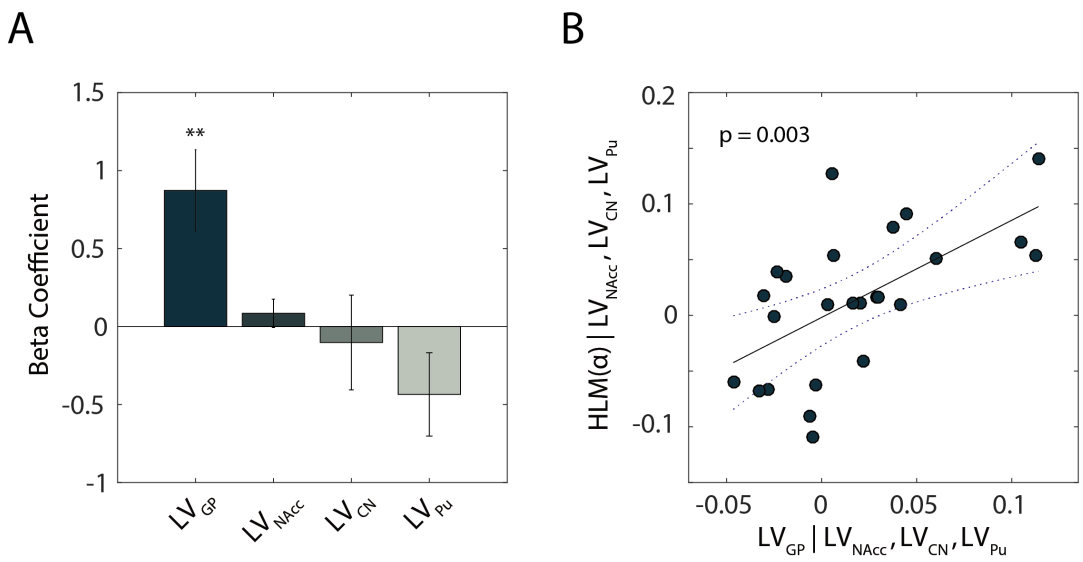

Figure 4. Lateralization of individual basal ganglia structures in relation to alpha hemispheric lateralized modulation (HLM) in the task. (A) Bar plot displays the Beta coefficients associated with a linear model where LV values were defined as explanatory variables for HLM(α). Error bars indicate standard error of the mean. Asterisks denote statistical significance; $^{**}p < .01$. (B) Partial regression plot showing the association between LV_{GP} and HLM(α), while controlling for the other regressors in the model in (A). Given equation(1) and (2), positive HLM(α) values indicate stronger modulation of alpha power in the right compared to the left hemisphere, and vice versa; Similarly, positive(or negative) LV_sindices denote greater right(or left) volume for a given substructure *s*. The dotted curves indicate 95% confidence bounds for the regression line, fitted on the plot in black.

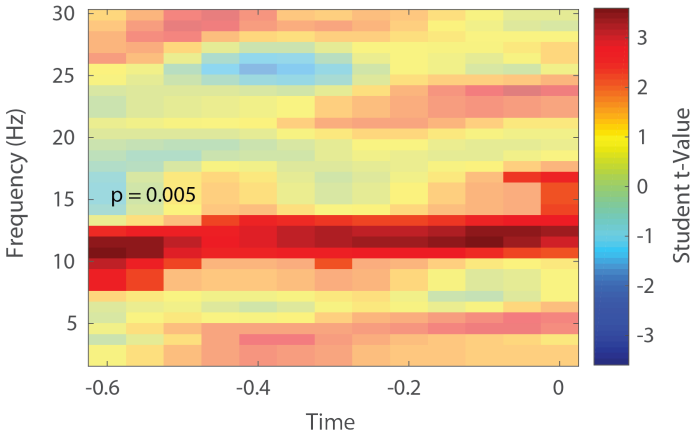

Figure 5. Time-frequency representation of regression coefficient t-statistics on the linear relationship between lateralized alpha modulation and LV_{GP} indices, averaged over ROIs (see Fig. 2A). The transparency mask highlights the significant time-frequency cluster, revealing a clear α-band-limited association between the variables across the full time window of interest (see Materials and Methods).

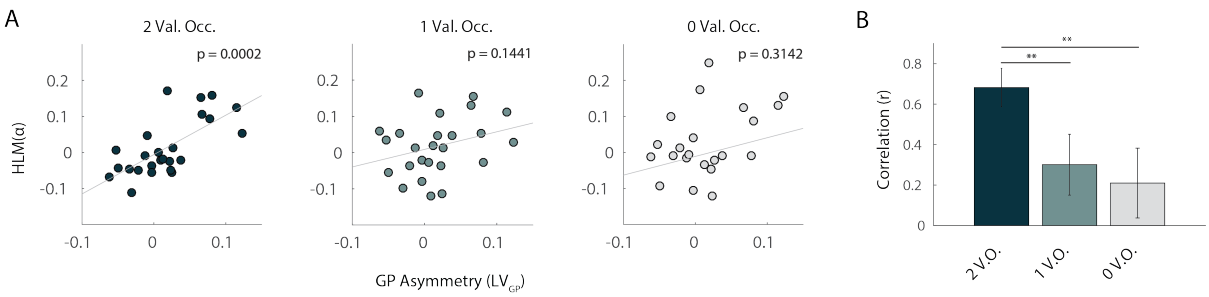

Figure 6. Linear association between GP volumetric asymmetry and alpha modulation asymmetry as a function of value occurrences in the task. (A) Correlation between GP volume lateralization and HLM(α), grouped accordingly to the amount of value-salient stimuli in the trials (see *Materials and Methods*). From left to right, respectively, two, one and zero value-saliency levels are displayed. GP asymmetry significantly explained HLM(α) only when value-salient stimuli featured as both target and distractors, irrespective of their valence ($r = .68$, significant at the $p < .001$ level after Bonferroni correction for three comparisons). (B) The association between HLM(α) and GP Lateralization increased as a function of reward in the task: the linear relationship was stronger when two rewarding stimuli were presented, when compared to conditions characterized by either one or zero reward pairings (95% CI [.106, .672] and [.125, .897], respectively for the two comparisons). This suggests that, when both target and distractor were associated with rewards or losses, participants exhibiting bigger GP volume in the left hemisphere than in the right hemisphere, were also better at modulating alpha oscillations in the left compared to the right hemisphere. Asterisks denote statistical significance; $^{**}p < .01$.